Studia Geotechnica et Mechanica, Vol. XXX, No. 1–2, 2008

LOCAL HEAVISIDE WEIGHTED MLPG MESHLESS METHOD APPROACH TO EXTENDED FLAMANT PROBLEM USING RADIAL BASIS FUNCTIONS

RAFAŁ OSSOWSKI

Gdańsk University of Technology, Department of Geotechnics and Applied Geology,
Narutowicza 11/12, 80-952 Gdańsk, Poland. ross@pg.gda.pl

Abstract: The meshless local Petrov–Galerkin (MLPG) method with Heaviside step function as the weighting function is applied to solve the extended Flamant problem. There are two different classes of trial functions considered in the paper: classical radial basis functions (RBF) as extended multiquadrics and compactly supported radial basis functions (CSRBF) as Wu and Wendland functions. The method presented is a truly meshless method based on a set of nodes only. This approach allows direct imposing of essential boundary conditions; moreover, no domain integration is needed and no stiffness matrix assembly is required. The solution of the extended Flamant problem is presented. The performance of RBFs and CSRBFs proposed is compared and the effect of the sizes of local subdomain and interpolation domain is studied. The results obtained show the accuracy and numerical performance of the method.

1. INTRODUCTION

During the past decade, the idea of using meshless methods for numerical solution of partial differential equations has received much attention as an alternative to the Finite Element and Boundary Element methods. The main reason for the development of meshless methods is to overcome some well-known drawbacks of FEM, such as: labour-intensive process of mesh-generation, poor derivative solutions, mesh distortion during large deformations, shear locking, etc. Using meshless methods one can get rid of, or at least alleviate the difficulty of, meshing and remeshing the entire domain; by only adding or deleting nodes in the desired area, instead.

The initial idea of meshless methods originates from the Smooth Particle Hydrodynamics (SPH) method by GINGOLD and MONAGHAN [6]. A serious study of meshless methods started after the publication of the Diffuse Element Method by NAYROLES et al. [10]. Several meshless methods have been proposed subsequently: Element-Free Galerkin method (EFG) by BELYTSCHKO et al. [4]; Reproducing Kernel Particle Method (RKPM) by LIU et al. [9]; hp-cloud method by DUARTE and ODEN [5]; the Partition of Unity Method (PUM) by BABUŠKA and MELENK [3]. All of these methods belong to a class of Galerkin methods; the major differences between them arise from the techniques used for interpolating the trial function. Although for the interpolation of the trial and test functions and the solution variables no mesh is required, it is inevitable that background cells should be used in these methods for the integration of the weak-form over the problem domain. Therefore, these methods are not ‘truly’ meshless.

A ‘truly’ meshless method, called the meshless local Petrov–Galerkin (MLPG) method, has been developed by ATLURI and ZHU [1], based on local subdomain equilibrium rather than on a global one. The MLPG method is based on a local weak form, and an integration method in regularly shaped local domains (such as rectangles and ellipsoids in 2D or spheres in 3D) is developed. An inherent feature of the method is its flexibility in choosing the size and the shape of the local sub-domain. The solution procedure does not require any element or mesh for either field interpolation or background integration.

The survey of the MLPG test functions can be found in ATLURI and SHEN [2]. The authors examined six different test functions, which lead to six different MLPG schemes. Among these, the one using the Heaviside function as the weighting function over a local subdomain proved to be highly promising because the integration difficulties can be removed, as it there was no domain integral (except body forces), and only a regular boundary integral along the edges of subdomains is involved.

The choice of optimal trial function is not a trivial task either. In fact, most of existing meshless methods have some inconveniences due to the interpolation schemes and corresponding numerical integration difficulties. The shape functions obtained from the common interpolation schemes (MLS, PUM, RKPM, etc.) in these meshless methods are non-polynomial functions and lack the delta function property, which causes certain difficulties, e.g., special treatments have to be introduced to impose essential boundary conditions, and/or modified numerical integration methods have to be employed.

Recently, radial basis functions (RBFs) (HARDY [7]) have been employed in solving partial differential equations. Excellent interpolation properties became the key to successful application of RBFs within meshless methods (LIU and GU [8], ATLURI and SHEN [2]). RBFs can be divided into two classes: globally supported RBFs which we refer to as classical radial basis functions and a new class of compactly supported radial basis functions (CSRBF) (WU [12], WENDLAND [11]). It should be noted that the shape functions based on all RBFs satisfy the delta function property.

2. INTERPOLATION USING RADIAL BASIS FUNCTIONS IN MLPG

The MLPG method is based on a local weak formulation of BVP. We consider two-dimensional problem of solid mechanics in the domain Ω, bounded by $\partial\Omega$ (figure 1):

$$\sigma_{ij,j} + \rho_i = 0\,, \tag{1}$$

where σ_{ij} is the Cauchy stress tensor, ρ_i represents the body force vector. The boundary conditions are given as follows:

$$t_i = \sigma_{ij} n_j = \bar{t}_i \quad \text{on the natural boundary } \partial\Omega_t , \tag{2}$$

$$u_i = \bar{u}_i \quad \text{on the essential boundary } \partial\Omega_u , \tag{3}$$

where n_j is the unit outward normal to the domain Ω, see figure 1. The local form of the BVP (1), over a local sub-domain Ω_s bounded by $\partial\Omega_s$, can be obtained using the weighted residual method:

$$\int_{\Omega_z} v_i (\sigma_{ij,j} + \rho_i) d\Omega = 0 , \tag{4}$$

where v_i is the Heaviside step function: $v_i(\mathbf{x}) = 1$ if $\mathbf{x}$ is in the sub-domain Ω_s, otherwise $v_i(\mathbf{x}) = 0$. This assumption leads to the following form of local equilibrium (4):

$$\int_{\partial\Omega_{sw}} t_i d\partial\Omega - \int_{\partial\Omega_{su}} t_i d\partial\Omega = \int_{\partial\Omega_{st}} \bar{t}_i d\partial\Omega + \int_{\partial\Omega_s} \rho_i d\Omega . \tag{5}$$

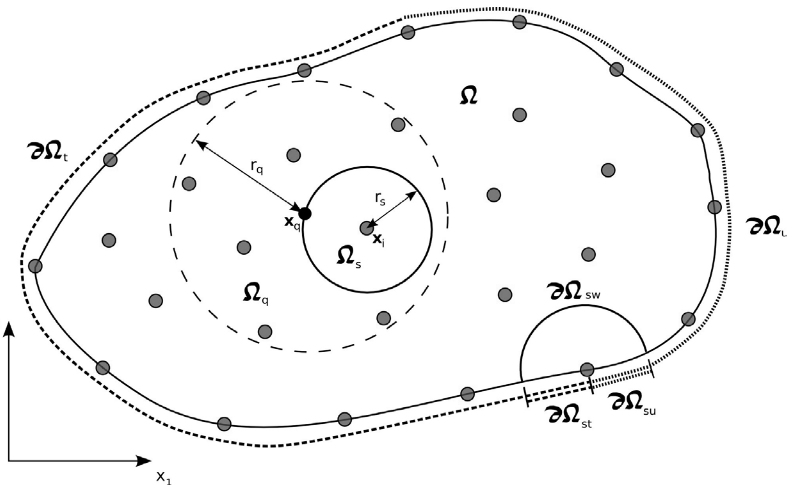

Fig. 1. The scheme of meshless local domains definition
– the support domain and interpolation domain of the node i

It has to be emphasized that equation (5) has a very simple form, containing only the regular boundary integrals along the boundaries of sub-domains and only one area integral of body forces. The local weak form is based on the local sub-domain Ω_s centred at the nodal point $\mathbf{x}_i$. The shapes of sub-domains can be chosen arbitrarily such as a rectangle or a circle (see figure 1).

For a node $\mathbf{x}_i$, there are two local domains: the test function domain (the same as the local sub-domain Ω_s) for $v_i(\mathbf{x}) = 1$ (size r_s) and the interpolation domain Ω_q for

$\mathbf{x}_q$ (size r_q). Figure 1 presents the local support domain Ω_s of a node $\mathbf{x}_i$ and the interpolation domain Ω_q for an integration point $\mathbf{x}_q$. These two domains are independent and defined by $r_s = \alpha_i d$ and $r_q = \alpha_q d$, respectively, where α_i and α_q are the coefficients and d is either the distance from the node i to its closest neighbouring node or the global boundary, whichever is smaller. As stated in the abstract, we are going to investigate the optimal values of α_i and α_q for a sample BVP, namely the Flamant problem.

In the present study, we use the interpolation scheme for the displacement function $u(\mathbf{x})$ defined in the domain Ω based on a set of nodes, as described by XIAO and MCCARTHY [13] and XIAO [14]. The radial basis functions used in current survey are as follows:

• The first class – the classical RBFs are represented by the Extended Multiquadrics function:

$$f_i(r) = (r^2 + c^2)^\beta, \tag{6}$$

where c and β are the parameters of the function. In simulation presented, the values of $c = 2.5$ and $\beta = 1.03$ were chosen after XIAO and MCCARTHY [13].

• The second class contains compactly supported RBFs, namely WU [12] and WENDLAND [11] functions. All these functions are strictly positive definite in R^d for all d less than or equal to some fixed value and can be constructed in such a way as to have any desired amount of the smoothness $2k$.

We consider the following CSRBFs:

• Wu-C2:

$$f_i(r) = \left(1 - \frac{r}{\delta}\right)_+^5 \left(5\frac{r^4}{\delta^4} + 25\frac{r^3}{\delta^3} + 48\frac{r^2}{\delta^2} + 40\frac{r}{\delta} + 8\right). \tag{7}$$

• Wendland-C2:

$$f_i(r) = \left(1 - \frac{r}{\delta}\right)_+^4 \left(4\frac{r}{\delta} + 1\right). \tag{8}$$

• Wendland-C4:

$$f_i(r) = \left(1 - \frac{r}{\delta}\right)_+^6 \left(35\frac{r^2}{\delta^2} + 18\frac{r}{\delta} + 3\right), \tag{9}$$

where: $(\alpha)_+ = \alpha$ for $\alpha \geq 0$ and $(\alpha)_+ = 0$ for $\alpha < 0$ and δ is the support radius of the function f_i. In the present study, the value of $\delta = 1000$ was choosen for the Wu-C2 and Wendland-C2 functions and $\delta = 200$ for the Wendland-C4 function, according to XIAO [14]. It is obvious that for such big values of δ the support size of a single node covers the whole domain. In order to make the interpolation domain size more exactly localized, we set the δ value as a parameter and used fixed value of α_i in the same way as for classical RBFs.

3. THE GENERALIZED FLAMANT PROBLEM

In the present study, the benchmarking problem is the Flamant problem. A strip foundation on elastic soil is subjected to a uniform load q (figure 2).

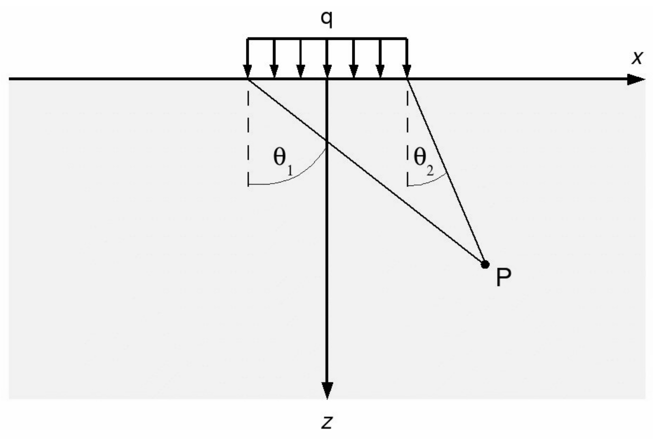

Fig. 2. The generalized Flamant problem

The analytical solution is a generalization of the Flamant problem. The values of the coefficients of stress tensor in the plane xz are given as follows:

$$\begin{aligned}
\sigma_{xx} &= \frac{q}{\pi}(\theta_1 - \theta_2 + \sin\theta_1 \cos\theta_1 - \sin\theta_2 \cos\theta_2), \\
\sigma_{zz} &= \frac{q}{\pi}(\theta_1 - \theta_2 - \sin\theta_1 \cos\theta_1 + \sin\theta_2 \cos\theta_2), \qquad (10) \\
\sigma_{xz} &= \frac{q}{\pi}(\cos^2\theta_2 - \cos^2\theta_1).
\end{aligned}$$

There is a half-space considered in the analytical solution; such an assumption leads to plane strain problem. The numerical solution under plane strain conditions imposes restrictions on the domain size.

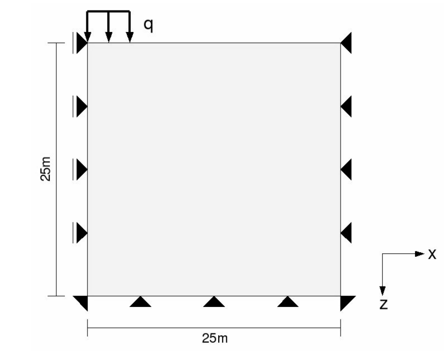

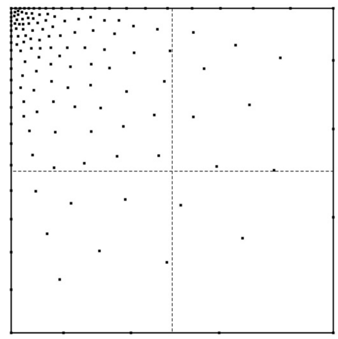

Fig. 3. The discretization domain for a sample Flamant problem and the node distribution

The proposed dimensions of the domain are: 50 m width and 25 m height, the foundation width is 2 m. The symmetry of the problem allows us to consider only a half of the domain, see figure 3. The numerical solution using MLPG leads to a straightforward implementation because of linear elastic model used.

4. RESULTS OF THE NUMERICAL SIMULATION

The problem domain is discretized into 151 nodes as shown in figure 3. The relative errors of σ_{zz} and σ_{xx} stress components at the point (x = 0.42, z = 0.88) are given in figures 4–6. The relative error is defined as follows: $e = \left| \sigma_{ij} - \underline{\sigma}_{ij} \right| / \underline{\sigma}_{ij}$, where $\underline{\sigma}_{ij}$ is the analytical stress. Figure 4 gives the results for classical RBF – the Extended Multiquadrics, figure 5 – the results for Wendland-C2 CSRBF, and figure 6 – the results for Wendland-C4 CSRBF. The Wu-C2 results were almost identical to those of Wendland-C2, so no plot is given.

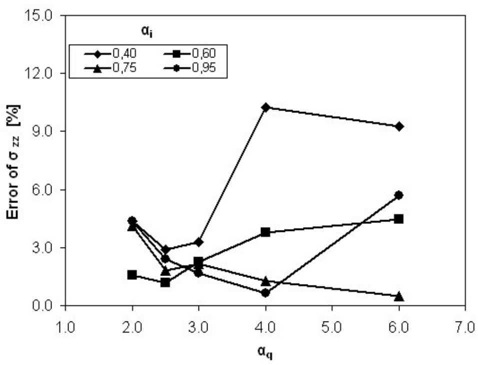

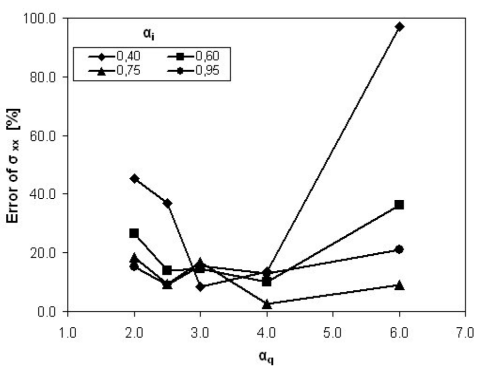

Fig. 4. Error of stress obtained for different values of the parameters α_q and α_i using the Extended Multiquadrics RBF

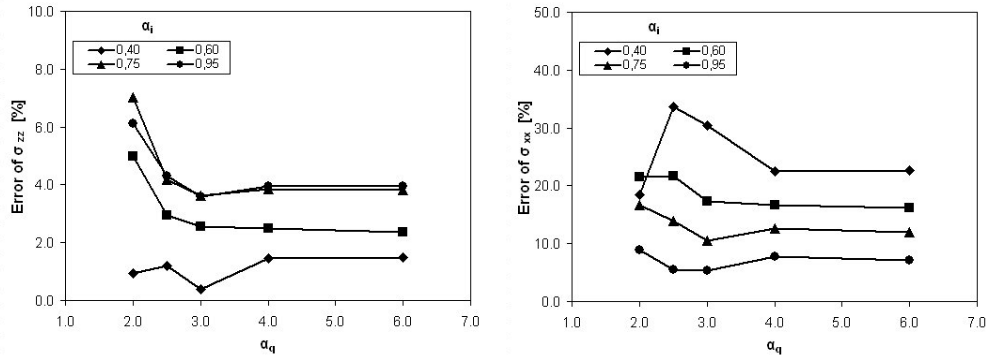

Fig. 5. Error of stress for different values of the parameters α_q and α_i using the Wendland-C2 RBF

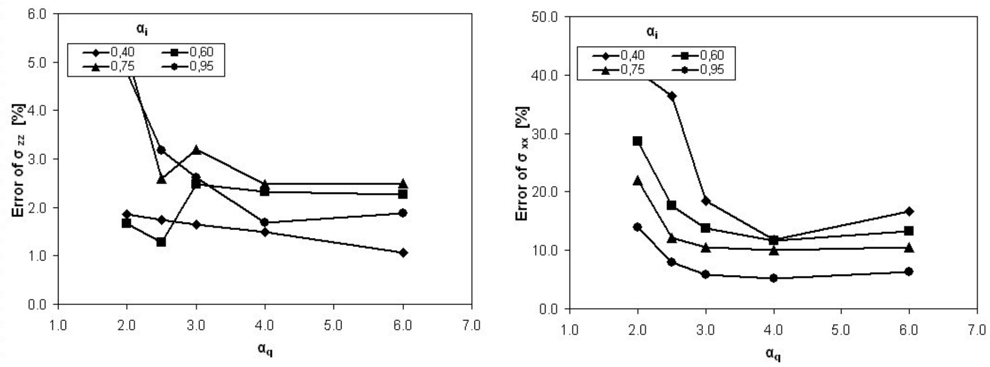

Fig. 6. Error of stress for different values of the parameters α_q and α_i the using Wendland-C4 RBF

For classical RBF the size of local domain $\alpha_i = 0.4$ was clearly too small. The best results are achieved for $\alpha_i = 0.75$ and $\alpha_i = 0.95$, while the optimal interpolation domain size α_q is 3.0. The results for CSRBF prove definitively that the accuracy is generally higher than that of classical RBFs interpolation. Slightly more accurate results are observed for the C4 interpolation than for the C2 one. It is interesting to observe for C2 a reverse order of α_i series in the case of σ_{zz} and σ_{xx}. Greater accuracy for σ_{zz} is achieved for smaller α_i, but the values of σ_{xx} are more accurate for higher values of α_i. In fact, a close look at the scale of both errors gives clear answer: for optimal results one should choose $\alpha_i = 0.75$ or more and α_q at least equal to 2.5, but no more than 6.0.

5. CONCLUSIONS

The results presented revealed a high usefulness of MLPG method in solving geomechanical problems. Two classes of RBFs, i.e., the classical ones and CSRBFs, were compared. The influence of the sizes of local subdomain and interpolation domain on the method accuracy was studied as the starting point for future and more precise investigations.

REFERENCES

[1] ATLURI S.N., ZHU T., *A new meshless local Petrov–Galerkin (MLPG) approach in computational mechanics*, Comput. Mech., 1998, Vol. 22.

[2] ATLURI S.N., SHEN S., *The meshless local Petrov–Galerkin (MLPG) method: a simple & less-costly alternative to the FE and BE methods*, Comput. Model. Eng. Sci., 2002, Vol. 3, No.1.

[3] BABUŠKA I., MELENK J., *The partition of unity method*, Int. J. Numer. Meth. Eng., 1997, Vol. 40.

[4] BELYTSCHKO T., LU Y.Y., GU L., *Element-free Galerkin methods*, Int. J. Numer. Meth. Eng., 1994, Vol. 37.

[5] DUARTE C.A., ODEN J.T., *An h-p adaptive method using clouds*, Comput. Meth. Appl. Mech. Eng., 1996, Vol. 139.

[6] GINGOLD R.A., MONAGHAN J.J., *Smooth particle hydrodynamics: theory and application to non-spherical stars*, Mon. Not. Roy. Astron. Soc., 1977, Vol. 181.

[7] HARDY R.L., *Multiquadratic equations of topography and other irregular surfaces*, J. Geophys. Res., 1971, Vol. 76.

[8] LIU G.R., GU Y.T., *A local point interpolation method for stress analysis of two-dimensional solids*, Struct. Eng. Mech., 2001, Vol. 11.

[9] LIU W.K., JUN S., ZHANG Y.F., *Reproducing kernel particle methods*, Int. J. Numer. Meth. Fluids, 1995, Vol. 20.

[10] NAYROLES B., TOUZOT G., VILLON P., *Generalizing the finite element method: diffuse approximation and diffuse elements*, Comput. Mech., 1992, Vol. 10.

[11] WENDLAND H., *Piecewise polynomial, positive definite and compactly supported radial basis functions of minimal degree*, Adv. Comput. Math., 1995, Vol. 4.

[12] WU Z., *Compactly supported positive definite radial basis functions*, Adv. Comput. Math., 1995, Vol. 4.

[13] XIAO J.R., MCCARTHY M.A., *A local Heaviside weighted meshless method for two-dimensional solids using radial basis functions*, Computational Mechanics, 2003, Vol. 31.

[14] XIAO J.R., *Local Heavside weighted MLPG meshless method for two-dimensional solids using compactly supported radial basis functions*, Comput. Methods Appl. Mech. Engrg., 2004, Vol. 193.